Inorganic Chemistry

ARTICLE

pubs.acs.org/IC

On the Magnetic Insulating States, Spin Frustration, and Dominant Spin Exchange of the Ordered Double-Perovskites Sr_2CuOsO_6 and Sr_2NiOsO_6: Density Functional Analysis

Chuan Tian,[†] Arief C. Wibowo,[‡] Hans-Conrad zur Loye,[‡] and Myung-Hwan Whangbo*[,†]

[†]Department of Chemistry, North Carolina State University, Raleigh, North Carolina 27695-8204, United States

[‡]Department of Chemistry and Biochemistry, University of South Carolina, Columbia, South Carolina 29208, United States

ABSTRACT: The ordered double-perovskites Sr_2MOsO_6 (M = Cu, Ni) consisting of 3d and 5d transition-metal magnetic ions (M^{2+} and Os^{6+}, respectively) are magnetic insulators; the magnetic susceptibilities of Sr_2CuOsO_6 and Sr_2NiOsO_6 obey the Curie−Weiss law with dominant antiferromagnetic and ferromagnetic interactions, respectively, and the zero-field-cooled and field-cooled susceptibility curves of both compounds diverge below ∼20 K. In contrast, the available density functional studies predicted both Sr_2CuOsO_6 and Sr_2NiOsO_6 to be metals. We resolved this discrepancy on the basis of systematic density functional calculations. The magnetic insulating states of Sr_2MOsO_6 are found only when a substantially large on-site repulsion is employed for the Os atom, although it is a 5d element. The cause for the divergence between the zero-field-cooled and field-cooled susceptibility curves in both compounds and the reason for the difference in their dominant magnetic interactions were investigated by examining their spin exchange interactions.

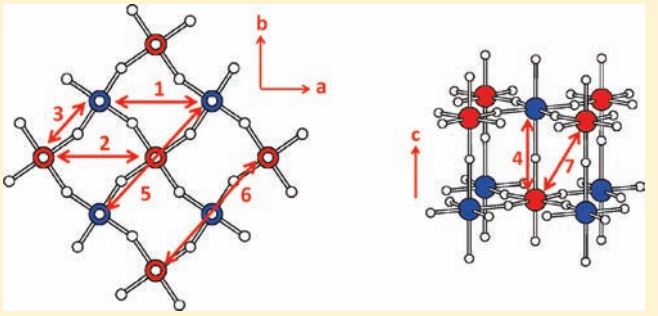

1. INTRODUCTION

The ordered double-perovskite Sr_2CuOsO_6,[1] crystallizing in a tetragonal space group $I4/m$, consists of corner-sharing CuO_6 and OsO_6 octahedra such that the CuO_6 and OsO_6 octahedra alternate in all three crystallographic directions with each Cu_4Os_4 cube containing a Sr^{2+} cation. The Cu−O−Os bridges in the layers parallel to the ab plane (hereafter the ∥ab layers) are bent (Figure 1a), but those along the c direction are linear (Figure 1b). In Sr_2CuOsO_6, the Cu and Os atoms are present as Cu^{2+} (d^9, S = 1/2) and Os^{6+} (d^2, S = 1) ions, respectively. Each CuO_6 octahedron exhibits a strong Jahn−Teller distortion associated with the $(t_{2g})^6(e_g)^3$ electron configuration of the Cu^{2+} ion, with two long Cu−O_{ax} bonds along the c direction and four short Cu−O_{eq} bonds in the ab plane [i.e., Cu−O_{ax} = 2.315 (× 2) Å, Cu−O_{eq} = 1.994 (× 4) Å]. Each OsO_6 octahedron displays a weak Jahn−Teller distortion associated with the $(t_{2g})^2$ electron configuration of the Os^{6+} ion, with two long Os−O_{ax} bonds along the c direction and four short Os−O_{eq} bonds in the ab plane [i.e., Os−O_{ax} = 1.928 (× 2) Å, Os−O_{eq} = 1.888 (× 4) Å]. As a consequence, the Cu−O_{eq} and Os−O_{eq} bonds of the Cu−O_{eq}−Os superexchange (SE) paths are considerably shorter in the ∥ab layers than the Cu−O_{ax} and Os−O_{ax} bonds of the Cu−O_{ax}−Os SE path along the c direction. In the 10 K structure of Sr_2NiOsO_6[2] each OsO_6 octahedron is axially elongated [i.e., Os−O_{ax} = 1.957 (× 2) Å, Os−O_{eq} = 1.907 (× 4) Å], whereas each NiO_6 octahedron shows a very weak axial elongation [i.e., Ni−O_{ax} = 2.040 (× 2) Å, Ni−O_{eq} = 2.023 (× 4) Å], although the Ni^{2+} (S = 1) ion is not Jahn−Teller active.

The magnetic susceptibility of Sr_2CuOsO_6[1] above 100 K is well described by a Curie−Weiss law with the Curie−Weiss temperature θ = −40 K, which shows the presence of dominant antiferromagnetic (AFM) interactions. The field-cooled (FC) and zero-field-cooled (ZFC) magnetic susceptibility curves of Sr_2CuOsO_6 diverge below ∼20 K, suggesting the presence of spin frustration. Sr_2NiOsO_6 exhibits somewhat different magnetic properties;[2] the magnetic susceptibility of Sr_2NiOsO_6 above 150 K is well described by a Curie−Weiss law with the Curie−Weiss temperature θ = 27 K, suggesting the presence of dominant ferromagnetic (FM) interactions. Nevertheless, the magnetic susceptibility shows a slight AFM downturn around 50 K and a deviation between the FC and ZFC susceptibility curves below ∼20 K. All these magnetic properties reveal that both Sr_2CuOsO_6 and Sr_2NiOsO_6 are magnetic insulators. Contrary to these experimental observations, the density functional theory (DFT) calculations by Song et al.[3,4] found both Sr_2CuOsO_6 and Sr_2NiOsO_6 to be metals.

A system with a partially filled band can be a metal or magnetic insulator depending on whether or not the width of the partially filled band is greater than the on-site repulsion U.[5,6] Unfortunately,

Received: January 28, 2011
Published: March 28, 2011

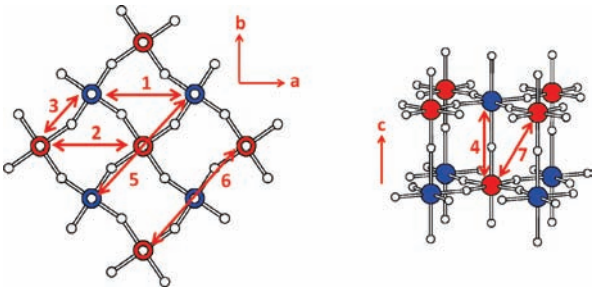

Figure 1. Schematic representation of the double-perovskite Sr_2CuOsO_6: (a) projection view, along the *c* direction, of an isolated ∥ *ab* layer of corner-sharing CuO_6 and OsO_6 octahedra. (b) Perspective view of two ∥ *ab* layers of corner-sharing CuO_6 and OsO_6 octahedra. The blue, red, and white circles represent the Cu, Os, and O atoms, respectively. The numbers 1−7 refer to spin exchange paths J_1−J_7, respectively.

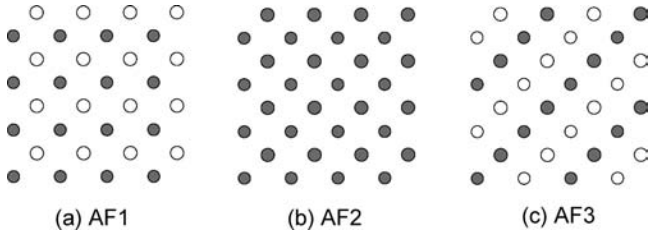

Figure 2. Schematic representations of the G-type and A-type antiferromagnetic spin arrangements of the double-perovskite Sr_2CuOsO_6 using the ordered spin arrangements of an isolated ∥ *ab* layer of Cu^{2+} and Os^{6+} ions: (a) In the G-type arrangement AF1, the given layer repeats antiferromagnetically along the *c* direction. (b) In the A-type arrangement AF2, the given layer repeats antiferromagnetically along the *c* direction. (c) In the A-type arrangement AF3, the given layer repeats ferromagnetically along the *c* direction. The filled and unfilled circles represent the up-spin and down-spin magnetic ion sites, respectively.

it is not possible at present to predict if such a system will be a metal or a magnetic insulator on the basis of first-principles DFT electronic structure calculations. The latter predict a magnetic insulator to be metallic when spin polarization is neglected and is often predicted to be a metal even if spin polarization is taken into consideration. To correct this failure, DFT calculations are carried out by adding the on-site repulsion *U* on the magnetic ions to enhance their spin polarization.[7] In such DFT plus U (DFT+U) calculations, the effective *U* value ($U_{eff} = U - J$, where *J* is the Stoner intra-atomic parameter) is an empirical parameter; systematic DFT+U calculations are necessary to establish the range of U_{eff} leading to a magnetic insulating state. For certain solids that have magnetic ions with spin−orbit coupling (SOC) located at high-symmetry sites, DFT+U plus SOC calculations are necessary to find a magnetic insulating state.[8−10]

Sr_2CuOsO_6 has two different magnetic ions (Cu^{2+} and Os^{6+}), and so does Sr_2NiOsO_6 (Ni^{2+} and Os^{6+}). Therefore, as found for the high-temperature magnetic structure of $RbMn[Fe(CN)_6]$ with Mn^{2+} ($S = 5/2$) and Fe^{3+} ($S = 1/2$) ions,[11] predicting a magnetic insulating state for Sr_2MOsO_6 (M = Cu, Ni) by DFT+U calculations is a nontrivial task. In the present work, we perform systematic DFT+U calculations to find the U_{eff} values of both M (= Cu, Ni) and Os [hereafter U_M and U_{Os}, respectively] necessary for reproducing the magnetic insulating states of Sr_2MOsO_6. Subsequently, we evaluate the spin exchange interactions of Sr_2CuOsO_6 and Sr_2NiOsO_6 to probe if the divergence between their FC and ZFC susceptibility curves below ∼20 K arises from the presence of spin frustration and why the dominant spin exchange interactions of the two compounds are opposite.

2. MAGNETIC INSULATING STATE AND ITS IMPLICATION

Our DFT calculations for Sr_2MOsO_6 (M = Cu, Ni) employed the frozen-core projector augmented wave (PAW) method encoded in the Vienna ab initio simulation packages (VASP)[12] and the generalized-gradient approximation (GGA)[13] with the plane-wave-cutoff energy of 400 eV and a set of 16 k points for the irreducible Brillouin zone. To examine the effect of electron correlation in the M 3d and Os 5d states, the DFT+U method[7] was employed with U_M = 3, 4, 5, and 6 eV and U_{Os} = 2, 3, and 4 eV.

A. Sr_2CuOsO_6. The magnetic orbital of a Cu^{2+} ion is an e_g orbital (i.e., x^2-y^2 due to the axial elongation of the CuO_6 octahedron), while those of an Os^{6+} (d^2) site are the t_{2g} orbitals (i.e., *xz* and *yz* due to the axial elongation of the OsO_6 octahedron). In Sr_2CuOsO_6, therefore, the overlap between the magnetic orbitals of the Cu^{2+} and Os^{6+} sites is zero for the linear Cu−O_{ax}−Os SE paths or practically zero for the bent Cu−O_{eq}−Os paths. Thus, to a first approximation, one might expect the Cu−O_{ax}−Os and Cu−O_{eq}−Os spin exchanges to be FM rather than AFM.[14−16] Thus, the G-type AFM structure (referred to as the AF1 state, Figure 2a) used for Sr_2CuOsO_6 by Song et al. in their DFT calculations,[3] in which every Cu−O−Os exchange has an AFM coupling, may not be appropriate.

An AFM spin exchange can arise from the Cu−O···O−Cu and Os−O···O−Os supersuperexchange paths within each ∥ *ab*-plane layer and from the Os−O···O−Os supersuperexchange paths between adjacent ∥ *ab*-plane layers (see Figure 1), because the magnetic orbitals in these exchange paths can overlap across their O···O contacts.[16] (The Cu−O···O−Cu interactions between adjacent ∥ *ab*-plane layers are not considered, their overlap through the O···O contact would be negligible.) These interactions can lead to the A-type AFM structure (referred to as the AF2 state, Figure 2b) in which the Cu^{2+} and Os^{6+} spins are ferromagnetically coupled within each ∥ *ab*-plane layer, and such layers are antiferromagnetically coupled. Alternatively, the Cu^{2+} and Os^{6+} spins are ferromagnetically coupled within each layer parallel to the (110) plane, and such layers are antiferromagnetically coupled, leading to another A-type AFM structure (referred to as the AF3 state, Figure 2c). It is important to see if the A-type AFM state is more stable than the G-type AFM state and whether the A-type AFM state is magnetic insulating.

We examine the aforementioned questions in terms of DFT+U calculations for Sr_2CuOsO_6. For various magnetic oxides of Cu^{2+} ions, the U_{Cu} values of 4−6 eV have been used to describe their magnetic properties. In general, the orbitals of a 5d element are much more diffuse than those of a 3d element, so that one might expect the U_{Os} value to be smaller than that of Cu. Thus, in our DFT+U calculations for the AF1, AF2, and AF3 states of Sr_2CuOsO_6, we varied U_{Os} from 2 to 4 eV with U_{Cu} fixed at 3, 4, 5, and 6 eV. Results of our calculations, summarized in Table 1, show that these states are all metallic when U_{Os} is smaller than 4 eV. With U_{Os} = 4 eV, the AF1 state remains metallic but both AF2 and AF3 states become magnetic insulating. In addition, the AF2 state becomes more stable than the AF1 and AF3 states. The need to use a substantially large U_{Os} in producing a magnetic insulating state for Sr_2CuOsO_6 indicates that the d electrons of the Os^{6+} ions of Sr_2CuOsO_6 are strongly localized,

dx.doi.org/10.1021/ic200167j |*Inorg. Chem.* 2011, 50, 4142–4148

Table 1. Relative Energies ΔE (in meV per two FUs) of the Three Ordered Spin States of Sr_2CuOsO_6 Determined from The DFT+U Calculations As a Function of the U_{Cu} and U_{Os} Values (in eV)[a]

	G type (AF1)		A type (AF2)		A type (AF3)	
(U_{Cu}, U_{Os})	ΔE	gap	ΔE	gap	ΔE	gap
(4,2)	0	no	120	no	133	no
(5,2)	0	no	55	no	140	no
(4,3)	60	no	0	no	26	no
(5,3)	0	no	57	no	87	no
(3,4)	23	no	0	yes	45	no
(4,4)	37	no	0	yes	52	no
(5,4)	50	no	0	yes	45	yes
(6,4)	60	no	0	yes	48	yes

[a] Whether each state is metallic (no band gap) or magnetic insulating (nonzero band gap) is also indicated, where "no" and "yes" refer to the absence and presence of a band gap, respectively.

which in turn means that the Os 5d orbitals are contracted due to the high oxidation state of the Os^{6+} ions. This reasoning is consistent with the fact that the Os−O bonds are considerably shorter than the Cu−O bonds in Sr_2CuOsO_6 [i.e., Os−O = 1.888 (× 4) and 1.928 (× 2) Å vs Cu−O = 1.994 (× 4) and 2.315 (× 2) Å].

B. Sr_2NiOsO_6. The positive Curie−Weiss temperature of Sr_2NiOsO_6 shows the presence of dominant FM interactions, but the magnetic susceptibility downturn below ∼50 K indicates the presence AFM interactions. To identify the preferred spin arrangement for Sr_2NiOsO_6, we examined the FM structure as well as three AFM structures, namely, G type, A type (the AF2 state), and C type (in which the FM chains made up of the Ni−O−Os exchange paths along the *c* direction are antiferromagnetically coupled). Results of our DFT+U calculations with U_{Ni} = 3 − 6 eV and U_{Os} = 4 eV are summarized in Table 2, which shows that the FM spin arrangement is most stable among the four states examined. This finding is consistent with the positive Curie−Weiss temperature of Sr_2NiOsO_6 but does not explain the magnetic susceptibility downturn below ∼50 K. To examine a possible cause for the latter as well as the difference between Sr_2NiOsO_6 and Sr_2CuOsO_6 in their dominant spin exchange interactions, it is necessary to evaluate the spin exchange interactions of Sr_2NiOsO_6 and Sr_2CuOsO_6.

3. SPIN EXCHANGE INTERACTIONS

To better understand the magnetic properties of Sr_2MOsO_6 (M = Cu, Ni), we examine the seven spin exchange interactions J_1−J_7 defined in Figure 1. The geometrical parameters associated with these exchange paths are listed in Table 3. To evaluate these interactions, we consider the relative energies of the eight ordered spin states, i.e., the AF1−AF7 states (see Figure 3) in addition to the FM state. The relative energies of these states calculated by performing DFT+U calculations with U_M = 6 eV and U_{Os} = 4 eV are summarized in Figure 3.

To extract the values of J_1−J_7, we express the total spin exchange interaction energies of the eight ordered spin states in terms of the spin Hamiltonian, $\hat{H} = -\Sigma_{i<j} J_{ij}\hat{S}_i \cdot \hat{S}_j$, where J_{ij} = J_1−J_7 is the spin exchange constant for the interaction between the spins $\hat{S}_i$ and $\hat{S}_j$ at sites *i* and *j*, respectively. By applying the

Table 2. Relative Energies ΔE (in meV per two FUs) of the Four Ordered Spin States of Sr_2NiOsO_6 Determined from the DFT+U Calculations As a Function of the U_{Co} and U_{Os} Values (in eV)[a]

	G-type AFM		A-type AFM		C-type AFM		FM	
(U_{Ni}, U_{Os})	ΔE	gap	ΔE	gap	ΔE	gap	ΔE	gap
(3, 4)	220	yes	87	yes	132	yes	0	yes
(4, 4)	198	yes	52	yes	115	yes	0	yes
(5, 4)	178	yes	59	yes	99	yes	0	yes
(6, 4)	159	yes	45	yes	85	yes	0	yes

[a] Whether each state is metallic (no band gap) or magnetic insulating (nonzero band gap) is also indicated, where "no" and "yes" refer to the absence and presence of a band gap, respectively.

energy expression obtained for spin dimers consisting of two spin sites with N_1 and N_2 unpaired spins (i.e., N_1 = 1 for Cu^{2+} and N_2 = 2 for Os^{6+} and N_1 = N_2 = 2 for Ni^{2+} and Os^{6+}),[17] the total spin exchange energies, per two formula units (FUs), of the eight ordered spin states are written as

$$
\begin{aligned}
E_{FM} &= (-4J_1 - 4J_5)(N_1^2/4) + (-4J_2 - 4J_6 - 8J_7)(N_2^2/4) \\
&\quad + (-8J_3 - 4J_4)(N_1N_2/4) \\
E_{AF1} &= (-4J_1 - 4J_5)(N_1^2/4) + (-4J_2 - 4J_6 - 8J_7)(N_2^2/4) \\
&\quad + (+8J_3 + 4J_4)(N_1N_2/4) \\
E_{AF2} &= (-4J_1 - 4J_5)(N_1^2/4) + (-4J_2 - 4J_6 + 8J_7)(N_2^2/4) \\
&\quad + (-8J_3 + 4J_4)(N_1N_2/4) \\
E_{AF3} &= (4J_1 - 4J_5)(N_1^2/4) + (4J_2 - 4J_6)(N_2^2/4) \\
&\quad + (-4J_4)(N_1N_2/4) \\
E_{AF4} &= (-2J_1 - 2J_5)(N_1^2/4) + (-4J_2 - 4J_6 - 8J_7)(N_2^2/4) \\
&\quad + (-6J_3 - 3J_4)(N_1N_2/4) \\
E_{AF5} &= (-4J_1 - 4J_5)(N_1^2/4) + (-4J_6)(N_2^2/4) \\
&\quad + (-4J_3 - 2J_4)(N_1N_2/4) \\
E_{AF6} &= (-2J_1)(N_1^2/4) + (-2J_2)(N_2^2/4) \\
&\quad + (-4J_3)(N_1N_2/4) \\
E_{AF7} &= (-2J_1 - 2J_5)(N_1^2/4) + (-2J_2 - 2J_6 + 4J_7)(N_2^2/4) \\
&\quad + (+2J_3 - 2J_4)(N_1N_2/4)
\end{aligned}
$$

Thus, by mapping the relative energies of the eight ordered spin states determined from DFT+U calculations onto the corresponding relative energies determined from the above expressions, we obtain the values of J_1−J_7. It should be noted from the energy expression for the FM state that there occur two J_3 and J_7 exchanges for every one of the remaining spin exchanges. This has an important consequence, as will be discussed below.

The two magnetic ions Cu^{2+} (S = 1/2) and Os^{6+} (S = 1) of Sr_2CuOsO_6 have different spin moments. Thus, in comparing the relative strengths of the spin exchanges between different spin sites, it is more meaningful to use the effective spin exchanges $J_{ij}^{eff} = S_iS_jJ_{ij} = N_iN_jJ_{ij}/4$, where $J_{ij} = J_1$−J_7. For Sr_2NiOsO_6, $J_{ij}^{eff} = J_{ij}$ because $S_i = S_j = 1$ for Ni^{2+} and Os^{6+}. The J_1^{eff}−J_7^{eff} values of Sr_2CuOsO_6 and Sr_2NiOsO_6 are listed in Table 4.

The J_1^{eff}−J_7^{eff} values of Sr_2CuOsO_6 show that the spin exchanges within each $\parallel ab$ layer are dominated by the Cu−O_{eq}−Os exchange J_3^{eff}, which is FM. Although J_5^{eff} is slightly greater than J_3^{eff} in magnitude, the effect of J_3^{eff} is stronger than that

dx.doi.org/10.1021/ic200167j |*Inorg. Chem.* 2011, 50, 4142–4148

Table 3. Geometrical Parameters Associated with the Spin Exchange Paths $J_{ij} = J_1 - J_7$ (in meV) of Sr_2MOsO_6 (M = Cu, Ni)

		Sr_2CuOsO_6	Sr_2NiOsO_6
J_1	M−O···O−M	O···O = 2.670(× 2) Å	O···O = 2.697(× 2) Å
J_2	Os−O···O−Os	O···O = 2.820(× 2) Å	O···O = 2.860(× 2) Å
J_3	M−O−Os	∠Cu−O−Os = 158.1°, Cu−O = 1.994 Å, Os−O = 1.888 Å	∠Ni−O−Os = 162.7°, Ni−O = 2.023 Å, Os−O = 1.907 Å
J_5	M−O···O−M	O···O = 3.775 Å	O···O = 3.815 Å
J_6	Os−O···O−Os	O···O = 3.988 Å	O···O = 4.045 Å
J_4	M−O−Os	∠Cu−O−Os = 180.0°, Cu−O = 2.315 Å, Os−O = 1.928 Å	∠Ni−O−Os = 180.0°, Ni−O = 2.040 Å, Os−O = 1.957 Å
J_7	Os−O···O−Os	O···O = 3.055(× 2) Å	O···O = 2.860(× 2) Å

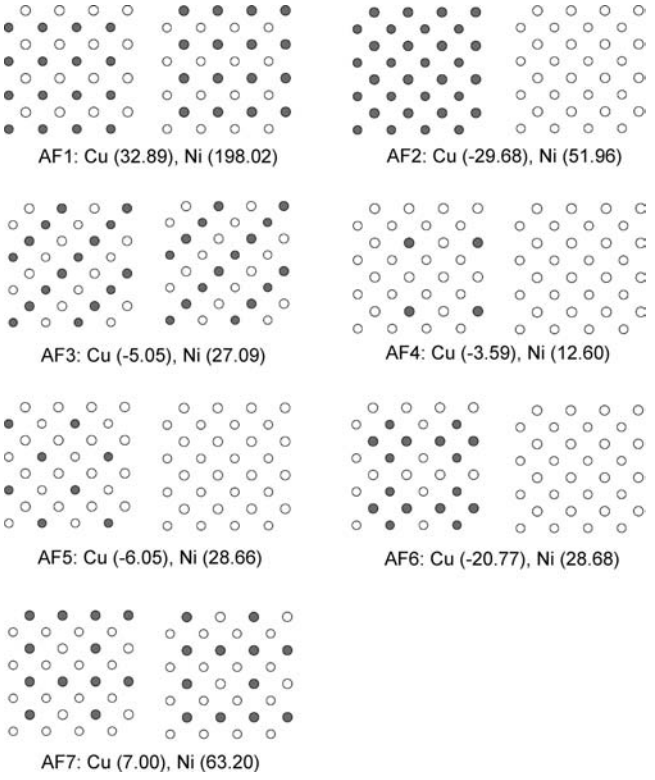

Figure 3. Spin arrangements in the AF1−AF7 states of Sr_2MOsO_6 (M = Cu, Ni) used to evaluate the J_1-J_7 values. In each state, the two ∥ *ab* layers with the given ordered spin arrangements alternate along the *c* direction. In the AF3 state, the two ∥ *ab* layers have the same spin arrangement. In the FM state (not shown), the ∥ *ab* layer with the FM spin arrangement repeats ferromagnetically along the *c* direction. In each state of Sr_2MOsO_6 (M = Cu, Ni), the number in the parentheses refers to the relative energies with respect to the FM state (in meV per two FUs), which was obtained from the DFT+U calculations with U_M = 6 eV and U_{Os} = 4 eV.

of J_5^{eff} because there are two J_3^{eff} interactions for every one J_5^{eff} interaction. This leads to an FM spin order in each ∥ *ab* layer. The spin exchanges between adjacent ∥ *ab* layers are dominated by J_7^{eff}, which is AFM. The latter gives rise to an AFM coupling between adjacent ∥ *ab* layers. Consequently, Sr_2CuOsO_6 is expected to adopt the A-type AFM structure, AF2, as the most stable ordered spin arrangement. Nevertheless, from Figure 1 and Table 4, we note the presence of significant spin frustration in the (J_1, J_3, J_3) and (J_2, J_3, J_3) triangles, in the (J_3, J_3, J_5) segments within each ∥ *ab* layer, and in the (J_6, J_7, J_7) triangles between adjacent ∥ *ab* layers. This suggests that the divergence of the ZFC and FC

Table 4. Spin Exchange Parameters $J_{ij}^{eff} = S_iS_jJ_{ij}$ of Sr_2CuOsO_6 and Sr_2NiOsO_6 (in meV), where $J_{ij} = J_1 - J_7$, Determined from the DFT+U Calculations with U_{Cu} = 6 eV and U_{Os} = 4 eV

exchange path		Sr_2CuOsO_6	Sr_2NiOsO_6
within ∥ *ab* layer	J_1^{eff}	−0.97	−0.23
	J_2^{eff}	−1.42	−0.70
	J_3^{eff}	2.84	5.55
	J_4^{eff}	−2.87	−3.35
	J_6^{eff}	−0.60	0.00
between ∥ *ab* layers	J_4^{eff}	−1.56	8.70
	J_7^{eff}	−1.07	−2.72

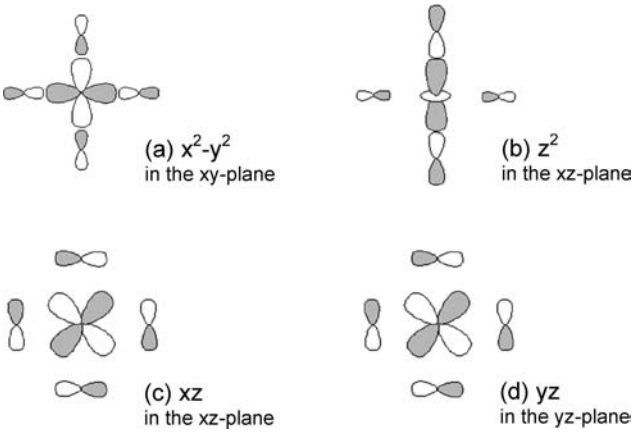

Figure 4. Schematic views of (a, b) the e_g-type magnetic orbitals of the M^{2+} ion and (c, d) the t_{2g}-type magnetic orbitals of the Os^{6+} ion in Sr_2MOsO_6 (M = Cu, Ni).

magnetic susceptibility curves of Sr_2CuOsO_6 below ∼20 K is caused by spin frustration.

In Sr_2NiOsO_6 the Ni−O_{ax}−Os spin exchange J_4^{eff} is by far the strongest, hence forming FM chains along the *c* directions. Between adjacent FM chains, there occur the Ni−O_{eq}−Os exchange J_3^{eff}, which is very strongly FM, and the Os−O···O−Os exchange J_7^{eff}, which is AFM. The next-nearest-neighbor FM chains interact by the Ni−O···O−Ni exchange J_5^{eff}, which is strongly AFM. The effect of J_5^{eff} cannot overcome that of J_3^{eff} because J_3^{eff} is stronger than J_5^{eff} in magnitude and there occur two J_3^{eff} interactions for every one J_5^{eff} interaction. The susceptibility downturn of Sr_2NiOsO_6 below 50 K might be related to the presence of the strong AFM interactions J_5^{eff} and J_7^{eff} between the FM chains made up of J_4^{eff}. Figure 1 and Table 4 show the

dx.doi.org/10.1021/ic200167j |*Inorg. Chem.* 2011, 50, 4142–4148

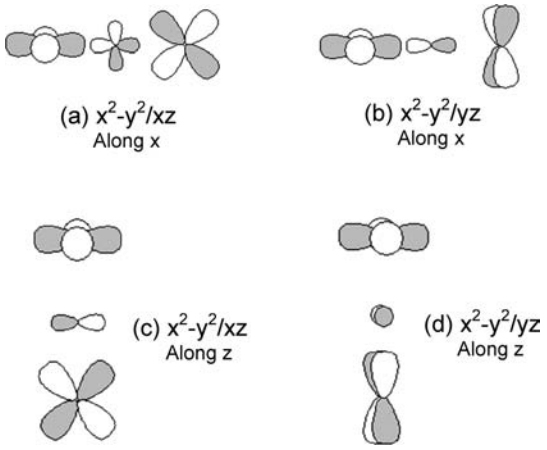

Figure 5. Orbitals involved in (a, b) the x^2-y^2/xz and x^2-y^2/yz spin exchange interactions of the M−O_{eq}−Os path and (c, d) those of the M−O_{ax}−Os path in Sr_2MOsO_6 (M = Cu, Ni). For simplicity, the orbital contributions unrelated to the exchange paths are not shown.

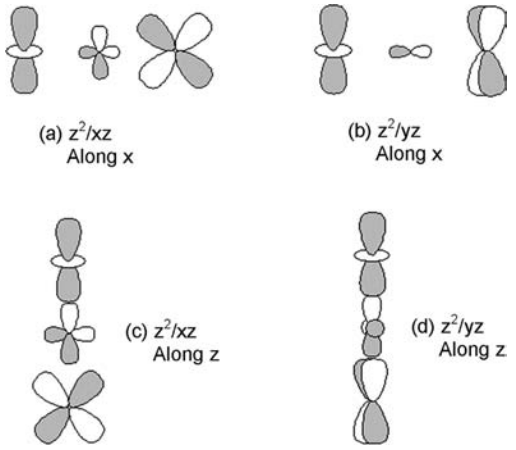

Figure 6. Orbitals involved in (a, b) the z^2/xz and z^2/yz spin exchange interactions of the Ni−O_{eq}−Os path and (c, d) those of the Ni−O_{ax}−Os path in Sr_2NiOsO_6. For simplicity, the orbital contributions unrelated to the exchange paths are not shown.

presence of significant spin frustration in the (J_3, J_3, J_5) segments within each ∥*ab* layer and in the (J_3, J_4, J_7) triangles between adjacent ∥*ab* layers. This suggests that the cause for the divergence of the ZFC and FC magnetic susceptibility curves of Sr_2NiOsO_6 below ∼20 K is spin frustration.

4. DISCUSSION

The striking differences between the spin exchanges of Sr_2CuOsO_6 and Sr_2NiOsO_6 are found for the M−O_{eq}−Os and M−O_{ax}−Os spin exchanges, namely, J_3^{eff} = 2.84 meV and J_4^{eff} = −1.56 meV in Sr_2CuOsO_6, whereas J_3^{eff} = 5.55 meV and J_4^{eff} = 8.70 meV in Sr_2NiOsO_6. As already pointed out, J_3^{eff} and J_4^{eff} involve the e_g orbitals of M^{2+} and the t_{2g} orbitals of Os^{6+}, so that they are expected to be FM, to a first approximation.[14−16] However, the Cu−O_{ax}−Os exchange J_4^{eff} of Sr_2CuOsO_6 is slightly AFM, whereas the Ni−O_{ax}−Os exchange J_4^{eff} of Sr_2NiOsO_6 is strongly FM. In contrast, the M−O_{eq}−Os exchange J_3^{eff} is FM for both Sr_2CuOsO_6 and Sr_2NiOsO_6 but is stronger for Sr_2NiOsO_6. To account for these differences, we note that a spin exchange J between two spin sites i and j, described by the magnetic orbitals ϕ_i and ϕ_j, respectively, is written as $J = J_F + J_{AF}$. The FM component J_F becomes stronger with increasing the overlap density distribution $\phi_i\phi_j$, while the AFM component J_{AF} becomes stronger with increasing the overlap integral $\langle\phi_i|\phi_j\rangle$. The magnetic orbitals of the Cu^{2+}, Ni^{2+}, and Os^{6+} ions of Sr_2MOsO_6 (M = Cu, Ni) are depicted in Figure 4. Each Cu^{2+} ion has the magnetic orbital x^2-y^2 (Figure 4a), each Ni^{2+} ion has the magnetic orbitals x^2-y^2 and z^2 (Figure 4a and 4b), and each Os^{6+} ion has the magnetic orbitals xz and yz (Figure 4c and 4d). In the e_g magnetic orbital(s) of each M^{2+}, the metal 3d orbitals make σ^*-antibonding interactions with the 2p orbitals of its first-coordinate O atoms. In the t_{2g} magnetic orbitals of Os^{6+}, the metal 5d orbitals make π^*-antibonding interactions with the 2p orbitals of its first-coordinate O atoms. For the M−O_{eq}−Os and M−O_{ax}−Os exchange paths, therefore, the overlap integrals of the e_g magnetic orbital(s) of M^{2+} with the t_{2g} magnetic orbitals of Os^{6+} are zero, so that the J_{AF} components of their exchanges (J_3^{eff} and J_4^{eff}, respectively) are zero to a first approximation. Thus, we need to examine only their J_F components.

Let us first consider Sr_2CuOsO_6. For the sake of simplicity, it will be assumed that the Cu−O_{eq}−Os exchange path is linear along the x direction. Then, the J_F component of the Cu−O_{eq}−Os exchange is given by the x^2-y^2/xz and x^2-y^2/yz overlap densities. For the x^2-y^2/xz interaction, both the x^2-y^2 and xz magnetic orbitals have an O 2p orbital contribution at the bridging atom O_{eq} (Figure 5a), so that the x^2-y^2/xz overlap density is nonzero, hence making J_F nonzero. For the x^2-y^2/yz interaction, the x^2-y^2 magnetic orbital has an O 2p orbital contribution at O_{eq} but the yz orbital does not (Figure 5b), so that the x^2-y^2/yz overlap density is zero, hence making its J_F zero. For the Cu−O_{ax}−Os exchange, both the x^2-y^2/xz and the x^2-y^2/yz interactions have no overlap density because the x^2-y^2 magnetic orbital has no O 2p contribution at the O_{ax} atom (Figure 5c and 5d). Thus, the J_F term is nonzero for the Cu−O_{eq}−Os exchange but is zero for the Cu−O_{ax}−Os exchange. This explains why the Cu−O_{eq}−Os exchange J_3^{eff} is FM but the Cu−O_{ax}−Os exchange J_4^{eff} is not in Sr_2CuOsO_6.

For each Ni^{2+} ion of Sr_2NiOsO_6, the z^2 orbital is also a magnetic orbital. Thus, in examining the J_F components of the Ni−O_{eq}−Os and Ni−O_{ax}−Os exchanges in Sr_2NiOsO_6 it is necessary to consider the z^2/xz and z^2/yz overlap densities in addition to the x^2-y^2/xz and x^2-y^2/yz overlap densities discussed above. For the Ni−O_{eq}−Os exchange, the z^2/xz interaction has a nonzero overlap density but the z^2/yz interaction does not (Figure 6a and 6b). For the Ni−O_{ax}−Os exchange, both the z^2/xz and z^2/yz interactions have a large overlap density because the z^2 magnetic orbital has a large O 2p contribution at O_{ax} (Figure 6c and 6d). By considering the overlap densities arising from both the x^2-y^2 and the z^2 magnetic orbitals, it is understandable why the Ni−O_{ax}−Os exchange J_4^{eff} is more strongly FM than the Ni−O_{eq}−Os exchange J_3^{eff} in Sr_2NiOsO_6 (8.7 vs 5.55 meV) and also why the Ni−O_{eq}−Os exchange J_3^{eff} of Sr_2NiOsO_6 is more strongly FM than the Cu−O_{eq}−Os exchange J_3^{eff} of Sr_2CuOsO_6 (5.55 vs 2.84 meV).

Finally, we comment on why the Cu−O_{ax}−Os exchange J_4^{eff} of Sr_2CuOsO_6 is not FM but slightly AFM. As discussed above, both the J_F and the J_{AF} terms of this J_4^{eff} exchange are practically zero so that one might expect J_4^{eff} to be nearly zero. However, it is calculated to be slightly AFM. The latter is possible if the Cu^{2+} ion of the Cu−O_{ax}−Os path interacts with the Os^{6+} ion indirectly through those Cu−O_{eq}···Sr^{2+}···O_{eq}−Os paths in which the magnetic orbitals of both the Cu^{2+} and the Os^{6+} ions

dx.doi.org/10.1021/ic200167j |*Inorg. Chem.* 2011, 50, 4142–4148

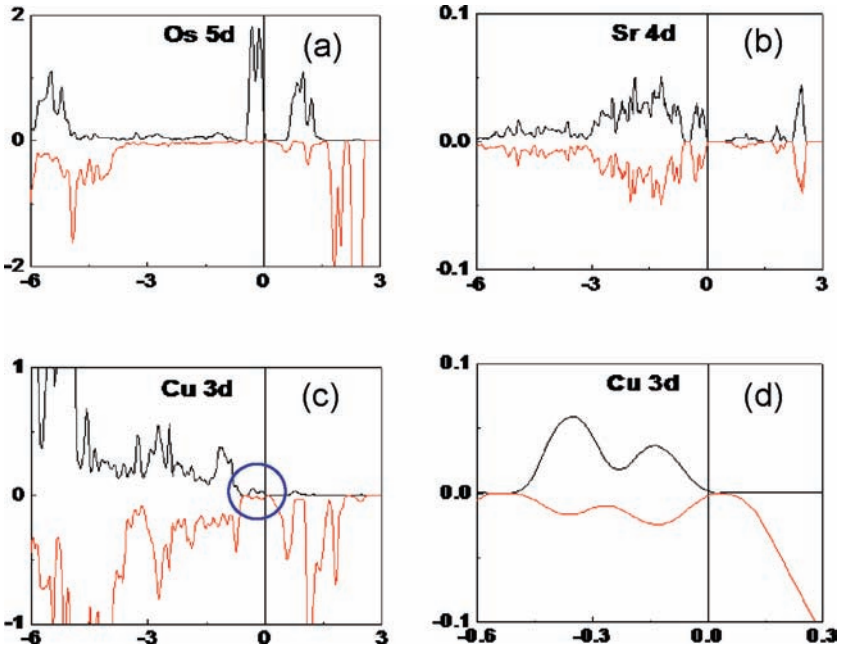

Figure 7. PDOS plots calculated for the (a) Os 5d, (b) Sr 4d, and (c, d) Cu 3d orbitals in the AF2 state of Sr_2CuOsO_6, where the horizontal axis is in units of eV and the vertical axis in states/eV/atom. The spin-up and spin-down states are represented by black and red curves, respectively, and their PDOS values are represented by positive and negative numbers, respectively. Figure 7d is a zoomed-in view of the circled region of Figure 7c.

have nonzero O 2p contributions on the O_{eq} atoms of the $O_{eq}\cdots Sr^{2+}\cdots O_{eq}$ linkage. In such paths, which involve the four Sr^{2+} cations surrounding each linear $Cu-O_{ax}-Os$ path, the empty 4d orbitals of Sr^{2+} can overlap with the magnetic orbital of Cu^{2+} and also with that of Os^{6+}. This is akin to the finding in Cs_2CuCl_4,[18] in which the Cs 6p orbitals of the Cs^+ ions strongly influence the spin exchange between two $(CuCl_4)^{2-}$ ions when the two $(CuCl_4)^{2-}$ anions and the Cs^+ cations lying between them have an inversion or a mirror plane of symmetry. We confirm the above possibility by calculating the plots of the projected density of states (PDOS) for the Os 5d, Cu 3d, and Sr 4d orbitals in the AF2 state of Sr_2CuOsO_6, which are shown in Figure 7. In the PDOS plot of the Os 5d states (Figure 7a), the states representing the magnetic orbitals of the Os^{6+} ion occur as two merged peaks immediately below the Fermi level. In this energy region of the Os^{6+} 5d states the Sr 4d states appear as two merged peaks (Figure 7b) and so do the Cu 3d states (Figure 7c and 7d). Furthermore, the Sr 4d and Cu 3d contributions in this energy region are comparable in magnitude. These observations are in support of the reasoning that the Cu^{2+} ion magnetic orbital of the $Cu-O_{ax}-Os$ path interacts with the Os^{6+} ion magnetic orbitals by overlapping with the Sr^{2+} ion 4d orbitals of the $Cu-O_{eq}\cdots Sr^{2+}\cdots O_{eq}-Os$ paths.

5. CONCLUDING REMARKS

To describe the magnetic insulating states of Sr_2CuOsO_6 and Sr_2NiOsO_6 by DFT+U calculations, it is necessary to employ a substantially large U_{Os} value. This indicates that the 5d orbitals of the Os^{6+} ion are strongly contracted due to the high oxidation state. The magnetic structure of Sr_2CuOsO_6 is best approximated by the A-type AFM arrangement (AF2) and that of Sr_2NiOsO_6 by the FM arrangement. However, significant spin frustration exists within each $\parallel ab$ layer and between adjacent $\parallel ab$ layers in both compounds. The latter is most likely responsible for the divergence of their ZFC and FC magnetic susceptibility curves below ~20 K. The crucial difference between the magnetic properties of Sr_2CuOsO_6 and Sr_2NiOsO_6 lies in their $M-O_{eq}-Os$ and $M-O_{ax}-Os$ spin exchanges, which arises ultimately from the fact that the Cu^{2+} ion has only one magnetic orbital (i.e., x^2-y^2) while the Ni^{2+} ion has two (i.e., x^2-y^2 and z^2). The $Ni-O_{ax}-Os$ exchange of Sr_2NiOsO_6 is strongly FM due to the z^2/xz and z^2/yz overlap densities. In contrast, the $Cu-O_{ax}-Os$ exchange of Sr_2CuOsO_6 is slightly AFM, which suggests indirect exchange interactions between the Cu^{2+} and the Os^{6+} ions through the $Cu-O_{eq}\cdots Sr^{2+}\cdots O_{eq}-Os$ paths.

AUTHOR INFORMATION

Corresponding Author
*E-mail: mike_whangbo@ncsu.edu.

ACKNOWLEDGMENT

Work at NCSU by the Office of Basic Energy Sciences, Division of Materials Sciences, U.S. Department of Energy, under Grant DE-FG02-86ER45259, and also by the computing resources of the NERSC center and the HPC center of NCSU. H. z.L. acknowledges support from the National Science Foundation via award DMR:0804209.

REFERENCES

(1) Lufaso, M.; Gemmill, W. R.; Mugavero, S. J.; Kim, S. J.; Lee, Y.; Vogt, T.; Loye, H. C. *J. Solid State Chem.* **2008**, *181*, 623.
(2) Macquart, R.; Kim, S.-S.; Gemmill, W. R.; Stalick, J. K.; Lee, Y.; Vogt, T.; zur Loye, H.-C. *Inorg. Chem.* **2005**, *44*, 9676.
(3) Song, W.; Wang, J.; Wu, Z. *Chem. Phys. Lett.* **2009**, *482*, 246.
(4) Song, W.; Zhao, E.; Meng, J.; Wu, Z. *J. Chem. Phys.* **2009**, *130*, 114707.
(5) Mott, N. F. *Metal-Insulator Transitions*; Barnes and Noble: New York, 1974.

(6) Whangbo, M.-H. *J. Chem. Phys.* **1979**, *70*, 4963.
(7) Dudarev, S. L.; Botton, G. A.; Savrasov, S. Y.; Humphreys, C. J.; Sutton, A. P. *Phys. Rev. B* **1998**, *57*, 1505.
(8) Xiang, H. J.; Whangbo, M.-H. *Phys. Rev. B* **2007**, *75*, 052407.
(9) Sarkar, S.; De Raychaudhury, M.; Dasgupta, I.; Saha-Dasgupta, T. *Phys. Rev. B* **2009**, *80*, 201101.
(10) Jeon, B. C.; Kim, C. H.; Moon, S. J.; Choi, W. S.; Jeong, H.; Lee, Y. S.; Yu, J.; Won, C. J.; Jung, J. H.; Hur, N.; Noh, T. W. *J. Phys.: Condens. Matter* **2010**, *25*, 345602.
(11) Tian, C.; Kan, E. J.; Lee, C.; Whangbo, M.-H. *Inorg. Chem.* **2010**, *49*, 3086.
(12) (a) Kresse, G.; Hafner, J. *Phys. Rev. B* **1993**, *47*, 558. (b) Kresse, G.; Furthmüller, J. *Comput. Mater. Sci.* **1996**, *6*, 15. (c) Kresse, G.; Furthmüller, J. *Phys. Rev. B* **1996**, *54*, 11169.
(13) Perdew, J. P.; Burke, K.; Ernzerhof, M. *Phys. Rev. Lett.* **1996**, *77*, 3865.
(14) Hay, P. J.; Thibeault, J. C.; Hoffmann, R. *J. Am. Chem. Soc.* **1975**, *97*, 4884.
(15) Kahn, O. *Molecular Magnetism*; VCH: New York, 1993.
(16) Whangbo, M.-H.; Koo, H.-J.; Dai, D. *J. Solid State Chem.* **2003**, *176*, 417.
(17) (a) Dai, D.; Whangbo, M.-H. *J. Chem. Phys.* **2001**, *114*, 2887. (b) Dai, D.; Whangbo, M.-H. *J. Chem. Phys.* **2003**, *118*, 29.
(18) Lee, C.; Kang, J.; Lee, K. H.; Whangbo, M.-H. *Inorg. Chem.* **2009**, *48*, 4185.